CHEMICAL ENGINEERING TRANSACTIONS
VOL. 94, 2022
A publication of AIDIC
The Italian Association of Chemical Engineering
Online at www.cetjournal.it
Guest Editors: Petar S. Varbanov, Yee Van Fan, Jiří J. Klemeš, Sandro Nižetić

ISBN 978-88-95608-93-8; **ISSN** 2283-9216
DOI: 10.3303/CET2294044

Heat Transfer Performance of Microfin Tubes and Three-Dimensional Heat Transfer Tubes

David J. Kukulka[a,*], Rick Smith[b], Wei Li[c]

[a] State University of New York College at Buffalo, 1300 Elmwood Avenue, Buffalo, New York, 14222 USA
[b] Vipertex, 658 Ohio Street, Buffalo New York. USA
[c] Zhejiang University, 866 Yuhangtang Road, Hangzhou 310027, PR China
kukulkdj@buffalostate.edu

Condensation heat transfer characteristics under different working conditions were studied to determine the heat transfer performance in horizontal, smooth and enhanced heat transfer tubes. Condensation heat transfer of these tubes was studied using R410A for a range of mass flow rates from 250 to 450 kg m^{-2} s^{-1} and a saturation temperature of 45 ℃. Visual flow pattern images and heat transfer performance for flow condensation are presented for the enhanced tubes and compared with that of a smooth tube for the same conditions. The condensation heat transfer coefficient enhancement ratio for the three dimensional tube is in the range 1.15 ~ 2.05, and the range of the microfin tube is 1.18 ~ 1.69. Additionally, it was found that the thermal conductivity of the smooth tube has a slight influence on its heat transfer performance, while a greater enhancement was found in the enhanced tubes. Stratified wavy flow (SW), intermittent flow (I), semi-annular flow (SA) and annular flow (A) were observed for the range of conditions investigated.
The heat transfer coefficient increased with an increase in mass velocity; as the mass flow rate increases, the turbulence of the liquid flow increases and the liquid film becomes thinner. This reduces thermal resistance and enhances heat transfer. Heat transfer performance for low mass velocities rise slowly; however the improvement of heat transfer performance at high mass flux rates is larger than that at low mass flux rates. Finally, better heat transfer performance is found in high thermal conductivity tubes with smaller diameters.

1. Introduction

Improving the heat transfer performance of heat transfer tubes is an important consideration to consider in order to save energy and realize "carbon neutrality". Enhanced heat transfer plays an important role in many industries (i.e. petrochemical, air conditioning, refrigeration, aerospace, etc.). Passive enhanced heat transfer technology with surface modification is an effective enhanced heat transfer technology to consider. Heat transfer is enhanced by disturbing the turbulence of the fluid, reducing the thickness of liquid film and/or enhancing the disturbance of the boundary layer.
Li et al. (2018) studied the condensation heat transfer performance of R410A in smooth, micro-fin, and enhanced three dimensional (3D) tubes; the Vipertex model 1EHT tubes showed good heat transfer performance demonstrating that the surface structure of dimples and petal arrays played an important role in condensation heat transfer. Sun et al. (2018) experimentally measured the condensation heat transfer coefficient (for copper 3D tubes) using R410A; they found the copper tubes produced 39-47 % higher heat transfer performance than that of stainless steel 3D tubes under the same conditions. Zheng et al. (2021) tested the condensation / evaporation heat transfer performance of R410A in different enhanced tubes; they found the performance of the enhanced tubes were 40 % to 73 % higher than smooth tubes.
It can be seen that there are several studies enhanced 3D tube heat transfer performance; experimental research is necessary to fill the gaps in this area. Previous studies on the flow patterns and heat transfer mechanism in micro-fin tubes and Vipertex series EHT, three-dimensional enhanced tubes were not sufficient. It is very important to investigate the heat transfer flow patterns. Flow patterns and condensation heat transfer

Paper Received: 02 April 2022; Revised: 17 April 2022; Accepted: 25 April 2022
Please cite this article as: Kukulka D.J., Smith R., Li W., 2022, Heat Transfer Performance of Microfin Tubes and -Three-Dimensional Heat Transfer Tubes, Chemical Engineering Transactions, 94, 265-270 DOI:10.3303/CET2294044

performance using R410A in horizontal smooth tubes (ST), micro-fin tubes (HX) and three dimensional enhanced tubes (Vipertex model 1EHT tubes) were studied. This visualization flow pattern study is unique.

2. Experimental Details

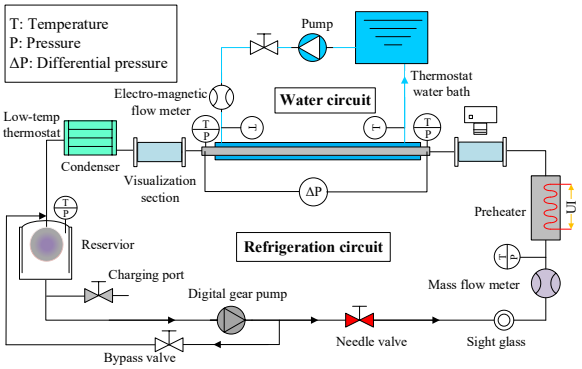

Figure 1: Schematic diagram of the experimental setup

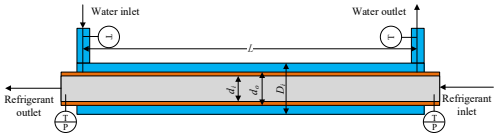

Figure 2: Schematic diagram of the heat exchange test section

(a) 1EHT (b) HX

Figure 3: Images of the enhanced surfaces: (a) Vipertex model 1EHT surface (b) HX surface

Table 1 Geometric parameters of the tested tubes

Parameter	Smooth tube	1EHT tube	HX tube
Material	Cu/SS	Cu/SS	Cu/SS
Outer diameter (mm)	9.52/12.7	9.52/12.7	9.52/12.7
Thickness (mm)	0.61	0.61	0.61
Length (m)	2	2	2
Dimple/fin height (mm)	-	0.19/1.71	0.25
Dimple/fin width (mm)	-	0.35/1.34	0.31
Dimple/fin pitch (mm)	-	4	0.8
Helix angle (°)	-	60	21
Surface Area enhancement ratio	1	1.34	1.44

Fig. 1 shows the system diagram of the experimental equipment. Accurate control and data monitoring of the refrigerant state under condensation or evaporation conditions is possible. The refrigerant cycle is made up of several sections: preheating, testing and cooling. Refrigerant is heated in the preheater to reach the inlet state;

in the test section; the refrigerant exchanges heat with the water on the outside of the tube. A visualization lens with a high-speed camera is installed at the outlet of the test section and used to observe the flow pattern of the refrigerant; finally, the refrigerant flows into the cooling section. Pressure and temperature sensors are installed at the inlet of the preheater and at the inlet/ outlet of the test section to monitor the state of the refrigerant.
Fig. 2 provides the details of the test section of this experiment. Deionized water flows through the annular region of the casing tube. The flow direction of deionized water is opposite to that of the refrigerant. The test section has an insulating layer in order to minimize heat loss. Fig. 3 shows the 3D surface structure of the 1EHT and the HX micro fin enhanced tubes. Table 1 provides the geometric characteristics of the enhanced tubes.

3. Analysis

After the temperature and pressure are constant for at least 15 minutes, the system is considered to be in steady-state. Reliability of the system is evaluated with the fluid properties obtained from Lemmon et al. (2010). According to the conservation of energy, the heat exchange quantity $Q_{ref,\ te}$ of the refrigerant in the test section is equal to the heat exchange quantity $Q_{w,te}$ of the annular water side and is given in Eq (1).

$$Q_{ref,te} = Q_{w,te} = c_{p,w,te} m_{w,te} \left(T_{w,te,out} - T_{w,te,in} \right) \tag{1}$$

where $c_{p,w,te}$ is the specific heat capacity of water; $m_{w,te}$ is the water mass flux in the test section; $t_{w,te,out}$ is the temperature of outlet water and $t_{w,te,in}$ is the temperature of inlet water in the test section. In addition, the heat flux of the refrigerant, $Q_{ref,te}$ is calculated using:

$$Q_{ref,te} = m_{ref} \left[H_{v,in} x_{in} - H_{v,out} x_{out} + \left(1 - x_{in} \right) H_{l,in} - \left(1 - x_{out} \right) H_{l,out} \right] \tag{2}$$

where m_{ref} is the refrigerant mass flux in the test section; $H_{v,in}$ and $H_{l,in}$ are the gaseous enthalpy and the liquid enthalpy of refrigerant in the test section inlet; $H_{v,out}$ and $H_{l,out}$ are the gaseous enthalpy and the liquid enthalpy of refrigerant in the test section outlet. Inlet vapor quality of the refrigerant x_{in} and outlet vapor quality x_{out} can be computed from Eq (3) and (4):

$$x_{in} = \frac{Q_{w,ph} - c_{p,ref} m_{ref} \left(T_{sat} - T_{ref,ph,in} \right)}{m_{ref} h_{lv}} \tag{3}$$

$$x_{out} = x_{in} - \frac{Q_{w,te}}{m_{ref} h_{lv}} \tag{4}$$

where, $Q_{w,\ ph}$ is the heat exchange of water in the preheating section; $c_{p,ref}$ is the specific heat capacity of condensed working fluid; T_{sat} is the saturation temperature of condensing working fluid; $T_{ref,ph,in}$ is the inlet temperature of condensation working fluid in preheating section; h_{lv} is the latent heat of vaporization.
The fouling thermal resistance in the experiment can be neglected. According to Newton's law of cooling, the condensation heat transfer coefficient, h_i , of the condensed fluid in the test tube can be represented as:

$$h_i = \frac{1}{A_i \left[\frac{LMTD}{Q_{te}} - \frac{1}{h_o A_o} - \frac{d_o \ln\left(d_o / d_i \right)}{2\lambda A_o} \right]} \tag{5}$$

where A_o is the heat exchange area at the annulus side of the test section; A_i is the heat exchange area in the test section tube; h_o is the heat transfer coefficient of the annulus water side of the test section; d_o and d_i are the outer diameter and inner diameter of the tested heat exchange tube; λ is the thermal conductivity of the tube material. Logarithmic average temperature difference, *LMTD, is* given by:

$$LMTD = \frac{\left(T_{w,te,in} - T_{ref,te,out} \right) - \left(T_{w,te,out} - T_{ref,te,in} \right)}{ln\left[\left(T_{w,te,in} - T_{ref,te,out} \right) / \left(T_{w,te,out} - T_{ref,te,in} \right) \right]} \tag{6}$$

where, $T_{ref,te,in}$ is the inlet temperature of the refrigerant in the test section; $T_{ref,te,out}$ is the outlet temperature of the refrigerant in the test section; $T_{w,te,in}$ and $T_{w,te,out}$ are temperatures of the inlet / outlet of the annular side. Heat transfer coefficient on the annular side (water) is predicted by the Gnielinski correlation (1976):

$$h_o = \frac{(f_w/2)(\mathrm{Re}_w - 1000)\mathrm{Pr}_w}{1+12.7(f_w/2)^{1/2}\left(\mathrm{Pr}_w^{2/3}-1\right)}\left(\frac{\mu_{bulk}}{\mu_w}\right)^{0.14}\cdot\frac{k_w}{d_h} \tag{7}$$

Fanning friction factor is given by Petukhov (1970):

$$f_w = \left(1.58\ln Re_w - 3.28\right)^{-2} \tag{8}$$

Moffat (1988) is used to analyze the uncertainty and is calculated using:

$$r(y) = \frac{1}{y}\sqrt{\sum_{i=1}^{n}\left(\frac{\partial y}{\partial x_i}\right)\sigma^2(x_i)} \tag{9}$$

The reliability and accuracy of the test equipment used in this experiment have been verified in Li et al. (2022).

4. Results and discussion

The condensation flow pattern using R410A was observed and recorded. Current results were analyzed and verified using the flow pattern diagram of Hajal et al (2003) with annular flow (A), semi-annular (SA), intermittent flow (I), stratified wavy flow (SW) and stratified flow (SF) being observed in this experiment.

Table 2 Accuracy of the primary parameters

Measurement Parameters	Accuracy
Diameter (mm)	± 0.05
Length (mm)	± 0.2
Temperature (K)	± 0.05
Pressure (range: 0 - 40 bar)	± 0.2 % of full scale
Differential pressure (range: 0 - 100 kPa)	± 0.05 % of reading
Water flow rate (range: 0 - 12 L min^{-1})	± 0.35 % of reading
Refrigerant flow rate (range: 0 - 90 kg h^{-1})	± 0.2 % of reading

Table 3 Accuracy of the calculated parameters.

Calculation Parameters	Accuracy
Mass flux (kg $m^{-2}s^{-1}$)	± 3.25 %
Heat flux (W m^{-2})	± 4.71 %
Vapor quality	± 6.30 %
Heat transfer coefficient (W m^{-2} k^{-1})	± 11.32 %

Fig. 4 shows the relationship between heat transfer coefficient (HTC) and mass flow rate. The condensation HTC of the copper and stainless steel heat transfer tubes (with an outer diameter of 12.7 mm) are shown. The results indicated that the HTC of a copper smooth tube was slightly higher than that of a stainless steel smooth tube. However, the HTC of the copper tube is significantly higher than that of stainless steel enhanced tubes. Fig. 5 shows the influence of the diameter of the tubes on the HTC is studied by comparing the HTC of the tubes with an outer diameter of 9.52 mm and 12.7 mm. The results show that at the same mass flow rate, the small diameter heat exchange tubes have a higher HTC.

Fig. 6 shows the geometric parameters of the two-phase flow taking place during condensation are presented; where, d_i is the inner diameter of the heat exchange tube; h_l is the height of condensed liquid; A_v is the cross-sectional area of refrigerant vapor in the heat exchange tube; A_l is the cross-sectional area occupied by refrigerant liquid (assuming that the liquid phase area, A_l , does not include the liquid condensed by the film on the upper part of the tube); θ_{strat} is the stratification angle; p_v is the circumference of the vapor at the top of the tube; and p_l is the circumference of the liquid at the bottom of the tube.

As shown in Fig. 7, the experimental observation results of a smooth copper tube with an outer diameter of 9.52 mm is compared with the predicted results of Hajal et al. (2003) for smooth tubes. In this study, semi-annular flow can be regarded as generalized annular flow; experimental results are basically consistent with the predicted results. Stratified wavy flow is shown at lower mass flow rates and lower vapor qualities. Semi-annular flow and annular flow occurs at higher mass flow rates and higher vapor qualities. By observing the flow pattern recorded using the visualization equipment; it can be found that with an increase of mass flow rate and vapor quality, the two-phase flow turbulence in the heat transfer tube becomes more intense and the mixing (at the junction of the gas phase and liquid phase) becomes more intense. In the condensation process the refrigerant in the heat transfer tube is subjected to the combined action of gravity, shear force and surface tension.

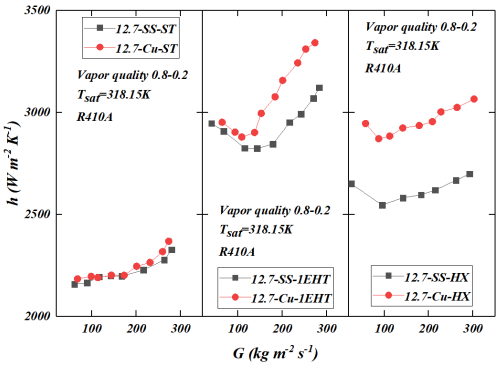

Figure 4: Comparison of condensation heat transfer coefficients inside 12.7-mm-OD copper and stainless steel tubes with various mass fluxes

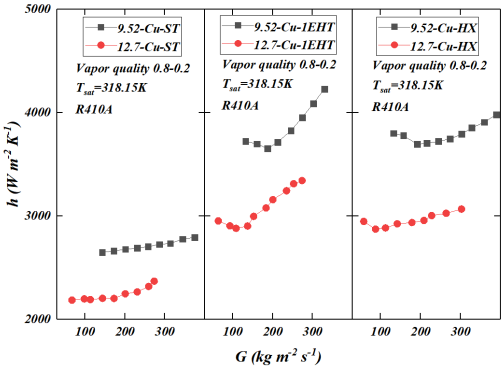

Figure 5: Condensation HTCs inside 9.52-mm-OD and 12.7-mm-OD copper tubes with various mass fluxes

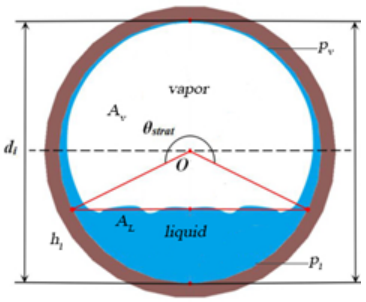

Figure 6: Geometric parameters of two-phase flow in heat exchange tube

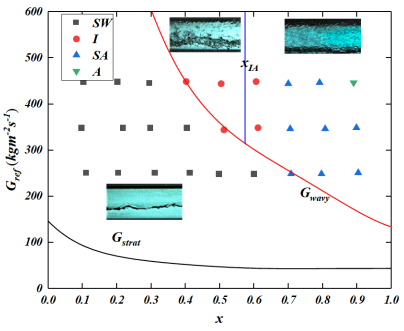

Figure 7: Flow patterns of smooth Cu-ST tube shown in the flow patterns map of Hajal et al. (2003)

At low mass flow rates and vapor qualities, gravity plays a dominant role; condensate is at the bottom of the heat transfer tube with the gas phase and liquid phase being stratified - the flow state is classified as stratified wavy flow. When the mass flow rates and vapor qualities increase the effects of shear force and the surface tension become more intense. This leads to an intensification of the mixing and produces a larger disorder at the gas-liquid interface. As a result, the increased surface tension of the refrigerant becomes more evenly distributed on the inner surface of the tube - forming an annular flow.

As shown in Fig. 8, the condensate flow pattern diagram of the 1EHT three-dimensional enhanced tube flow is shown and compared with the flow pattern diagram of smooth tube. It is concluded that the proportion of the stratified wavy flow is reduced; intermittent flow, semi-annular flow and annular flow are all generated being produced at lower vapor qualities.

Fig. 9 shows the flow pattern of flow condensation in the HX micro-fin tube; when compared with the 1EHT three-dimensional enhanced tube, the area of the stratified wavy flow is compressed; in addition intermittent flow, semi-annular flow and annular flow occurs at the condition of low vapor quality. This is a result of the fins

on the inner surface of the micro-fin tube having a certain upward stretching effect on the refrigerant along the wall surface, promoting the flow pattern conversion

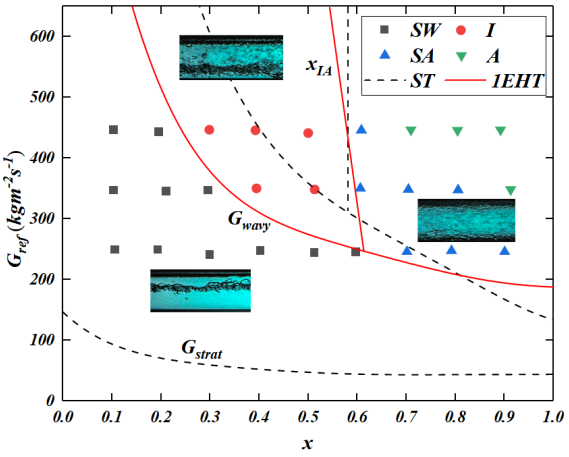

Figure 8: Flow patterns of the Cu-1EHT tube.

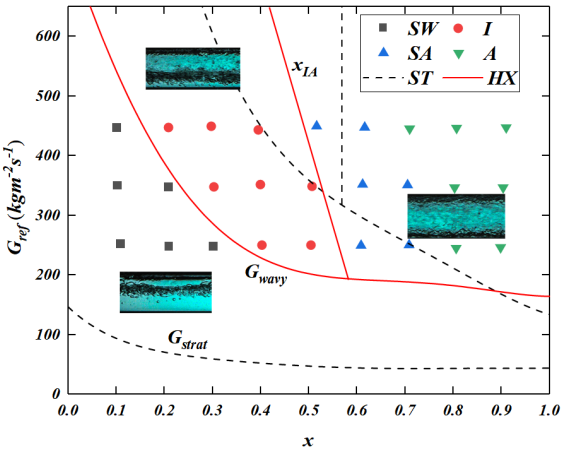

Figure 9: Flow patterns of the Cu-HX tube.

5. Conclusions

Experimental investigations on condensation heat transfer in horizontal smooth and enhanced tubes were conducted using R410A. HX micro-finned tubes and 1EHT enhanced tubes (copper and stainless steel) were evaluated with different diameters (9.52 mm and 12.7 mm). Condensation heat transfer using R410A in the enhanced tubes was studied. Observed flow patterns in the enhanced tubes are discussed and the flow pattern diagrams in the enhanced tubes were created. The following conclusions can be drawn:

1. It can be concluded that tubes produced of higher thermal conductivity material or using a smaller tube diameter will lead to better heat transfer performance. Heat transfer improvement (based upon thermal conductivity) of smooth tubes is limited; however, the influence on enhanced tubes is more significant.
2. Flow patterns observed include stratified wavy flow, intermittent flow, semi-annular flow and annular flow. In addition, the transition from stratified wavy flow to intermittent flow; and intermittent flow to annular flow in enhanced tubes occurs at a lower vapor quality. This is mainly influenced by the surface enhancing structure; this promotes the liquid being extended to the upper part of the tube.

References

Gnielinski, V., 1976, New Equations for Heat and Mass Transfer in Turbulent Pipe and Channel Flow, Int. J. Chem. Eng., 16(2): 8-16.

Hajal, J. E., Thome, J. R., Cavallini A., 2003, Condensation in horizontal tubes, part 1:two-phase flow pattern map, Int. J. Heat Mass Transf., 46(18), 3349-3363.

Lemmon, E. W., Huber, M. L., Mclinden, M. O., 2010, NIST Standard Reference Database 23: Reference Fluid Thermodynamic and Transport Properties-REFPROP. 9.0, NIST NSRDS.

LI, W., Wang, J.C., Guo, Y., Shi, Q.Y., He, Y., D.J. Kukulka, Luo, X., Kabelac, S., 2022, R410A flow condensation inside two dimensional micro-fin tubes and three dimensional dimple tubes. Int. J. Heat Mass Transf., 121910.

Li, W., Tang, W., Chen, J., Zhu, H., Kukulka, D.J., He, Y., Sun, Z., Du, J., Zhang, B., 2018, Convective condensation in three enhanced tubes with different surface modifications. Exp Therm Fluid Sci , 97, 79-88.

Moffat, R. J., 1988, Describing the uncertainties in experimental results, Exp. Therm.Fluid Sci., 1 3–17.

Petukhov, B. S., 1970, Heat Transfer and Friction in Turbulent Pipe Flow with Variable Physical Properties, Adv. Heat Transf., 6: 503-564.

Sun, Z.C., Li, W., Guo, R.H., He, Y., Kukulka, D.J., 2018, Condensation heat transfer in horizontal three dimensional two-layer two-side enhanced tubes, Int J Heat Mass Tran, 127, 141-145.

Zheng, B., Wang, J, Guo, Y, Kukulka, D.J., Tang, W.Y., Smith, R., Sun, Z.C., Li,W., 2021, An Experimental Study of In-Tube Condensation and Evaporation Using Enhanced Heat Transfer (EHT) Tubes, Energies, 14(4), 867-867.